

The Kuramoto model with inertia: from fireflies to power grids

Simona Olmi

Inria Sophia Antipolis Méditerranée Research Centre - Sophia Antipolis, France

Istituto dei Sistemi Complessi - CNR - Firenze, Italy



Pteroptix Malaccae



- A phase model with **inertia** has been introduced to mimic the synchronization mechanisms observed among the Malaysian fireflies **Pteroptix Malaccae**. These fireflies synchronize their flashing activity by entraining to the forcing frequency with almost zero phase lag. Usually, entrainment results in a constant phase angle equal to the difference between pacing frequency and free-running period as it does in **P. cribellata**.

(B. Ermentrout (1991), Experiments by Hanson, (1987))

Why introducing “inertia”?

■ First-order Kuramoto model

- It approaches too fast the partial synchronized state
- Infinite coupling strength is required to achieve full synchronization

■ Second-order Kuramoto model

- Synchronization is slowed down by inertia (**frequency adaptation**)
- Firstly proposed in biological context ([Ermentrout, \(1991\)](#))
- Used to study synchronization in disordered arrays of Josephson junctions ([Strogatz \(1994\)](#), [Tees et al. \(2005\)](#))
- Derived from the classical swing equation to study synchronization in power grids ([Filatrella et al. \(2008\)](#))

The Model

Kuramoto model with inertia

$$m\ddot{\theta}_i + \dot{\theta}_i = \Omega_i + \frac{K}{N} \sum_j \sin(\theta_j - \theta_i)$$

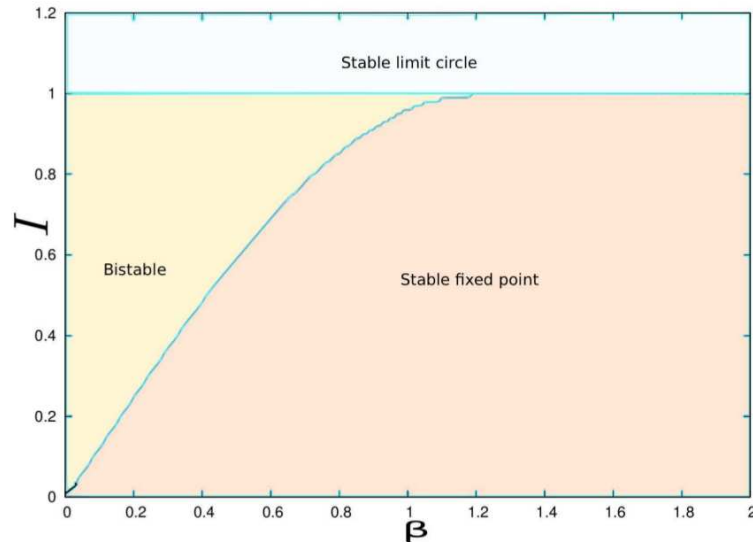
- θ_i is the instantaneous phase
- Ω_i is the natural frequency of the i -th oscillator with Gaussian distribution
- K is the coupling constant
- N is the number of oscillators

By introducing the complex order parameter $r(t)e^{i\phi(t)} = \frac{1}{N} \sum_j e^{i\theta_j}$

$$m\ddot{\theta}_i + \dot{\theta}_i = \Omega_i - Kr \sin(\theta_i - \phi)$$

$r = 0$ asynchronous state, $r = 1$ synchronized state

Damped Driven Pendulum



$$m\ddot{\theta}_i + \dot{\theta}_i = \Omega_i - Kr \sin(\theta_i)$$

$$I = \frac{\Omega_i}{Kr}$$

$$\beta = \frac{1}{\sqrt{mKr}}$$

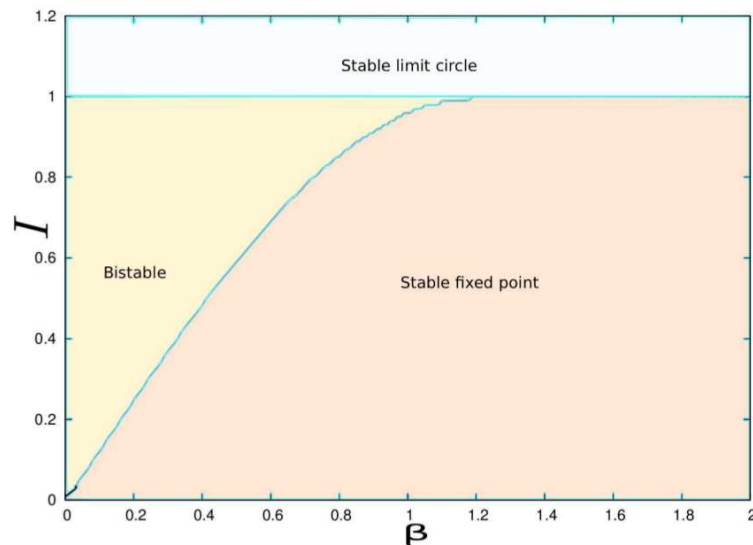
$$\ddot{\phi} + \beta\dot{\phi} = I - \sin(\phi)$$

- One node connected to the grid (the grid is considered to be infinite)
- Single damped driven pendulum
- Josephson junctions
- One-machine infinite bus system of a generator in a power-grid (Chiang, (2011))

Damped Driven Pendulum

$$\ddot{\phi} + \beta \dot{\phi} = I - \sin(\phi)$$

For sufficiently large m (small β)



- For small Ω_i two fixed points are present: a **stable node** and a **saddle**.

The linear stability is given by

$$J = \begin{pmatrix} 0 & 1 \\ -\cos \phi^* & -\beta \end{pmatrix}$$

$$\sigma_{1,2} = \frac{-\beta \pm \sqrt{\beta^2 - 4 \cos \phi^*}}{2}$$

- At large frequencies $\Omega_i > \Omega_P = \frac{4}{\pi} \sqrt{\frac{Kr}{m}}$ (i.e. $I > \frac{4\beta}{\pi}$) a **limit cycle** emerges from the saddle via a homoclinic bifurcation

- Limit cycle and fixed point coexists until $\Omega_i \equiv \Omega_D = Kr$ (i.e. $I = 1$), where a saddle node bifurcation leads to the **disappearance of the two fixed points**
- For $\Omega_i > \Omega_D$ (i.e. $I > 1$) only the **oscillating solution** is present

For small mass (large β), there is no more coexistence.
(Levi et al. 1978)

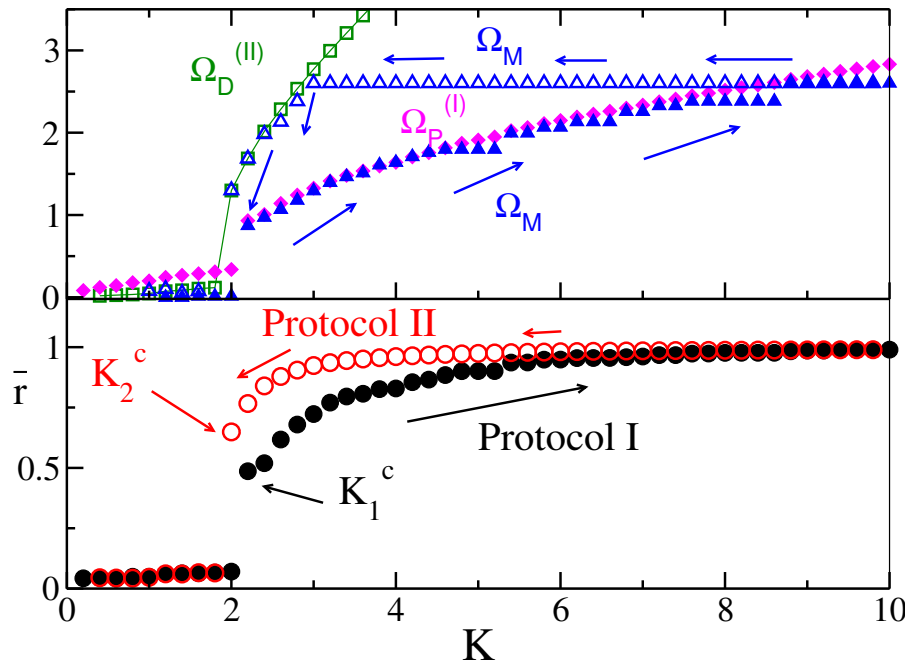
Simulation Protocols

Dynamics of N oscillators (first order transition and hysteresis)

■ Ω_M maximal natural frequency of the locked oscillators

■ $\Omega_P^{(I)} = \frac{4}{\pi} \sqrt{\frac{Kr}{m}}$

■ $\Omega_D^{(II)} = Kr$



$m = 2$

Protocol I: Increasing K

The system remains desynchronized until $K = K_c^1$ (filled black circles).

Ω_M increases with K following Ω_P^I .

Ω_i are grouped in small clusters (plateaus).

Protocol II: Decreasing K

The system remains synchronized until $K = K_c^2$ (empty black circles).

Ω_M remains stuck to the same value for a large K interval than it rapidly decreases to 0 following Ω_D^{II} .

Mean Field Theory (Tanaka et al. (1997))

$$m\ddot{\theta}_i + \dot{\theta}_i = \Omega_i - Kr \sin(\theta_i - \phi)$$

- by following Protocol I and II there is a group of **drifting** oscillators and one of **locked** oscillators which act separately
 - **locked** oscillators are characterized by $\langle \dot{\theta} \rangle = 0$ and are locked to the mean phase
 - **drifting** oscillators (with $\langle \dot{\theta} \rangle \neq 0$) are whirling over the locked subgroup (or below depending on the sign of Ω_i)
- **Drifting** and **locked** oscillators are separated by a certain frequency:
 - Following Protocol I the oscillators with $\Omega_i < \Omega_P$ are **locked**
 - Following Protocol II the oscillators with $\Omega_i < \Omega_D$ are **locked**
- These two groups contribute differently to the total level of synchronization in the system

$$r = r_L + r_D$$

Mean Field Theory (Tanaka et al. (1997))

Protocol I: $\Omega_P^{(I)} = \frac{4}{\pi} \sqrt{\frac{Kr}{m}}$

- All oscillators initially drift around its own natural frequency Ω_i
- Increasing K , oscillators with $\Omega_i < \Omega_P$ are attracted by the locked group
- Increasing K also Ω_P increases \Rightarrow oscillators with bigger Ω_i become synchronized
- The phase coherence r^I increases and Ω_i exhibits plateaus
- ! Depending on m the transition to synchronization may increase in complexity

Protocol II: $\Omega_D^{(II)} = Kr$

- Oscillators are initially locked to the mean phase and $r^{II} \approx 1$
- Decreasing K , locked oscillators are desynchronized and start whirling when $\Omega_i > \Omega_D$ and a saddle node bifurcation occurs

Ω_P, Ω_D are the synchronization boundaries

Mean Field Theory (Tanaka et al. (1997))

Total level of synchronization in the system: $r = r_L + r_D$

For the **locked** population the self-consistent equation is

$$r_L^{I,II} = Kr \int_{-\theta_{P,D}}^{\theta_{P,D}} \cos^2 \theta g(Kr \sin \theta) d\theta$$

where $\theta_P = \sin^{-1}(\frac{\Omega_P}{Kr})$, $\theta_D = \sin^{-1}(\frac{\Omega_D}{Kr}) = \pi/2$, $g(\Omega)$ frequency distribution.

The **drifting** population contributes to the total order parameter with a negative contribution

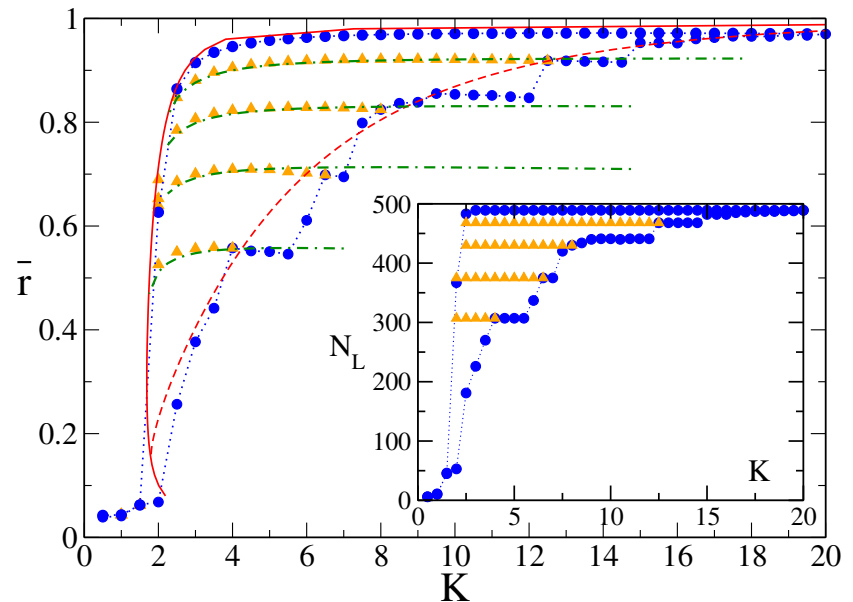
$$r_D^{I,II} \simeq -mKr \int_{-\Omega_{P,D}}^{\infty} \frac{1}{(m\Omega)^3} g(\Omega) d\Omega$$

The former equation are correct **in the limit of sufficiently large masses**

Hysteretic Behavior

Numerical Results for Fully Coupled Networks ($N = 500, m = 6$)

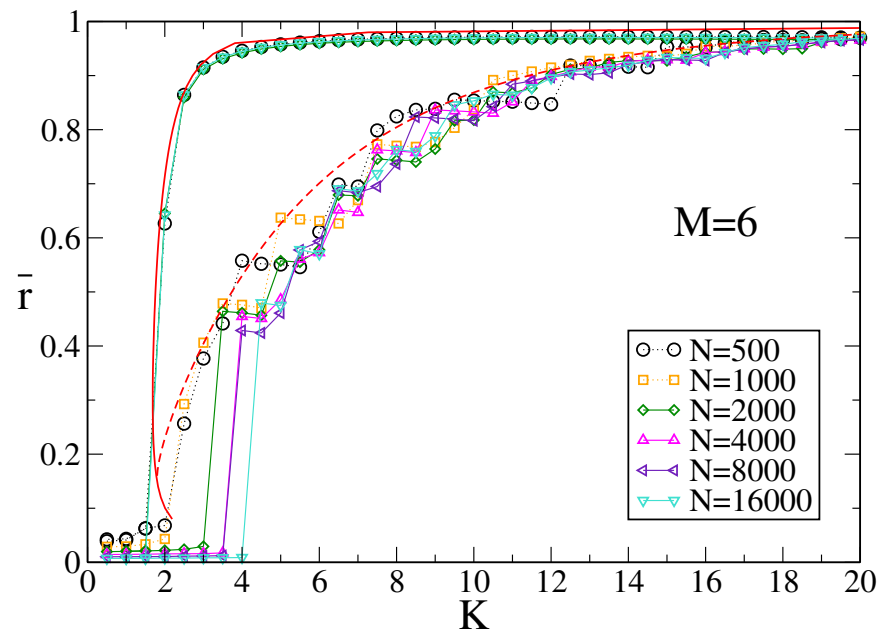
- The data obtained by following [protocol II](#) are quite well reproduced by the mean field approximation r^{II}
- The mean field estimation r^I does not reproduce the stepwise structure numerically obtained in [protocol I](#)
- Clusters of N_L locked oscillators of any size remain stable between r^I and r^{II}
- The level of synchronization of these clusters can be [theoretically](#) obtained by generalizing the theory of [Tanaka et al. \(1997\)](#) to protocols where Ω_M remains constant



(Olmi et al. (2014))

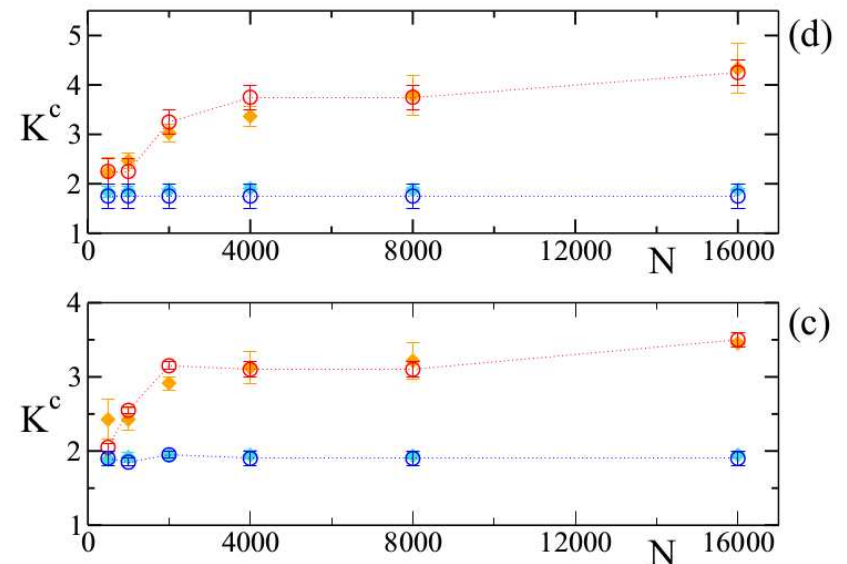
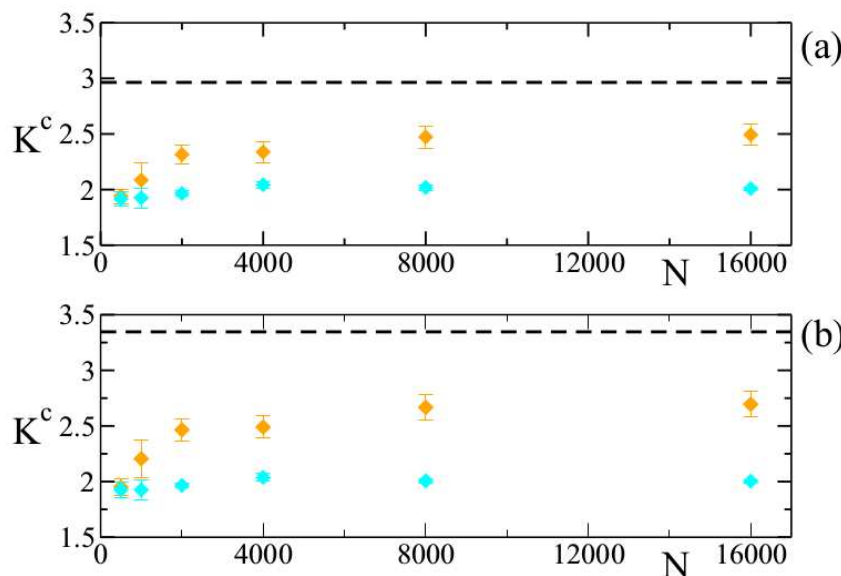
Finite Size Effects

- K_1^c is the transition value from asynchronous to synchronous state (following Protocol I)
- K_2^c is the transition value from synchronous to asynchronous state (following Protocol II)



Finite Size Effects (Olmi et al. (2014))

- a) $m = 0.8$, (b) $m = 1$, (c) $m = 2$ and (d) $m = 6$
- K_1^c (upper points) is strongly influenced by the size of the system
- K_2^c (lower points) does **not** depend heavily on N
- Good agreement between Mean Field and simulations is achieved for **small m**
- For **large m** the emergence of the secondary synchronization of drifting oscillators (i.e. **clusters of whirling oscillators**) is determinant



Dashed line $\rightarrow K_1^{MF}$ mean field value by [Gupta et al \(PRE 2014\)](#)

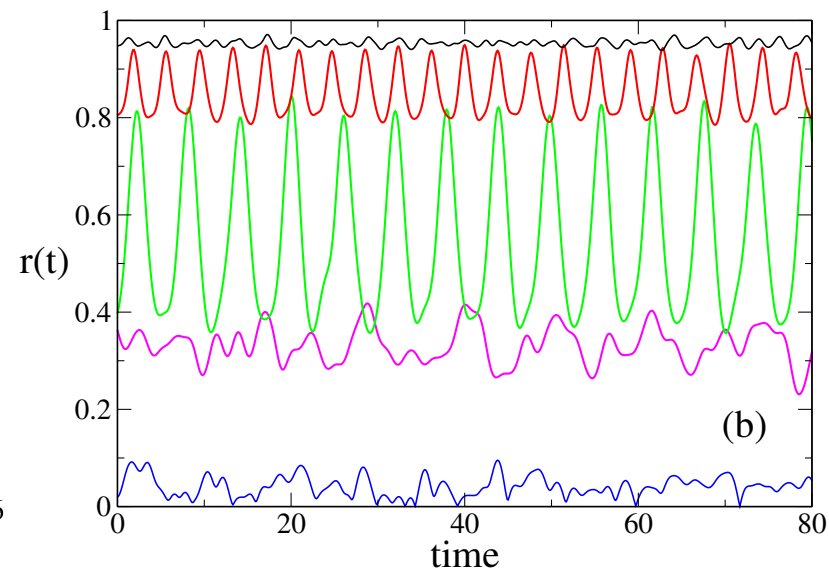
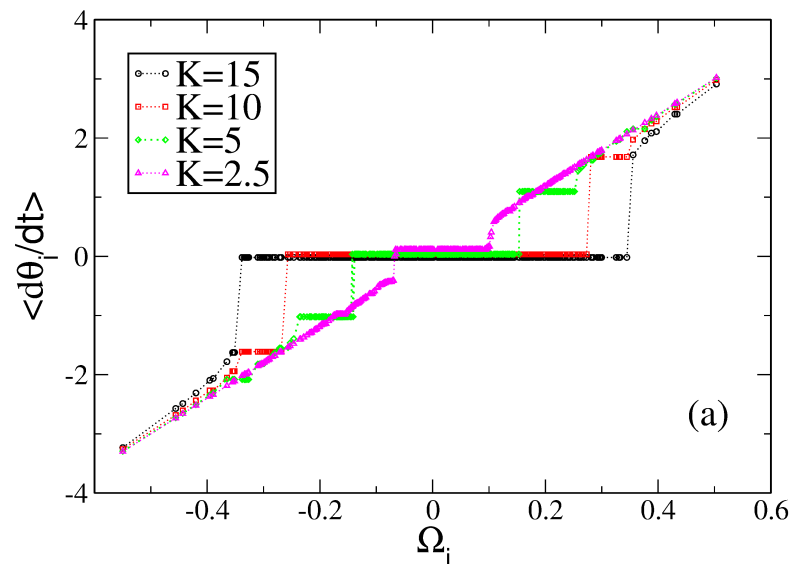
Drifting Clusters

For larger masses ($m=6$), the synchronization transition becomes more complex, it occurs via the emergence of clusters of **drifting oscillators**.

The partially synchronized state is characterized by the coexistence of

- a cluster of locked oscillators with $\langle \dot{\theta} \rangle \simeq 0$
- clusters composed by **drifting oscillators** with **finite average velocities**

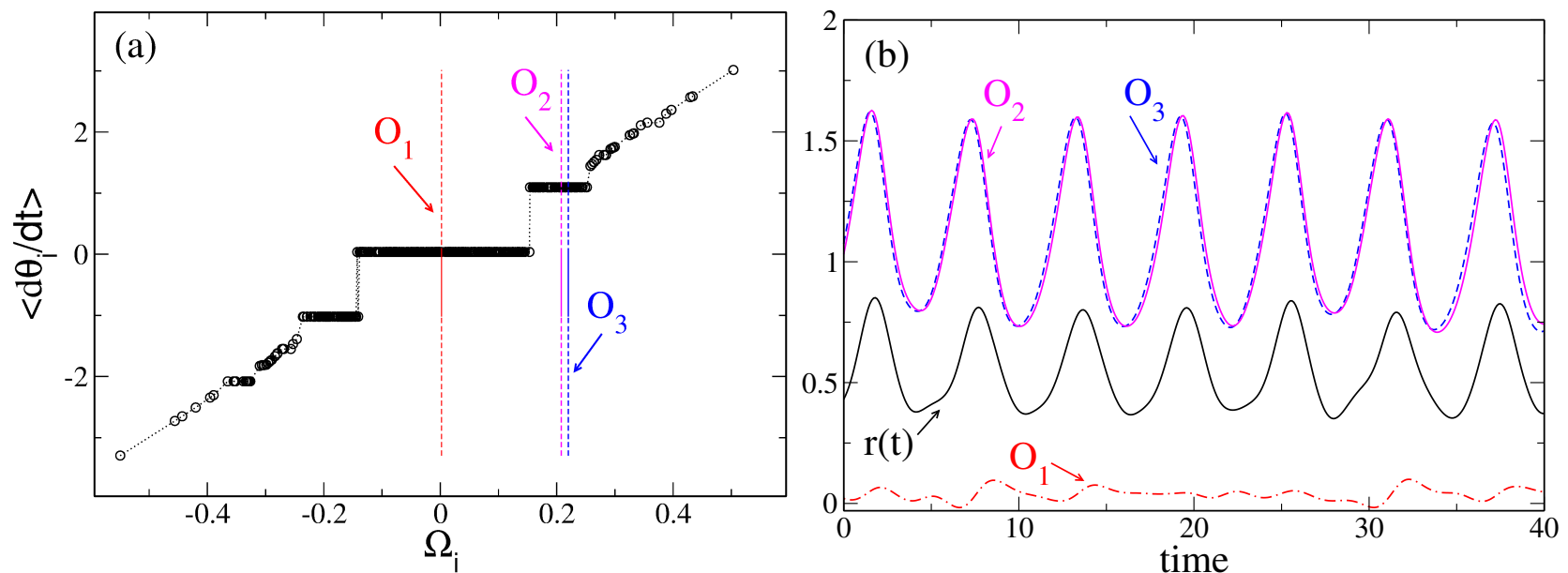
Extra clusters induce (periodic or quasi-periodic) oscillations in the temporal evolution of $r(t)$.



Drifting Clusters

If we compare the evolution of the instantaneous velocities $\dot{\theta}_i$ for 3 oscillators and $r(t)$ we observe that

- the phase velocities of O_2 and O_3 display **synchronized motion**
- the phase velocity of O_1 oscillates **irregularly** around zero
- the oscillations of $r(t)$ are **driven** by the periodic oscillations of O_2 and O_3



Linear Stability Analysis of the Asynchronous State

- Tool: **nonlinear Fokker-Planck** formulation for the evolution of the single oscillator distribution $\rho(\theta, \dot{\theta}, \Omega, t)$ for coupled oscillators with inertia and noise
- Critical coupling K_1^{MF} for an unimodal frequency distribution $g(\Omega)$ with width Δ

$$\frac{1}{K_1^{MF}} = \frac{\pi g(0)}{2} - \frac{m}{2} \int_{-\infty}^{\infty} \frac{g(\Omega) d\Omega}{1 + m^2 \Omega^2}$$

- If $g(\Omega)$ is Lorentzian $\Rightarrow K_1^{MF} = 2\Delta(1 + m\Delta)$
- If $g(\Omega)$ is Gaussian
 - the zero mass limit gives

$$K_1^{MF} = 2\Delta \sqrt{\frac{2}{\pi}} \left\{ 1 + \sqrt{\frac{2}{\pi}} m\Delta + \frac{2}{\pi} m^2 \Delta^2 + \sqrt{\left(\frac{2}{\pi}\right)^3 - \frac{2}{\pi} m^3 \Delta^3} \right\} + \mathcal{O}(m^4 \Delta^4)$$

- The limit $m\Delta \rightarrow \infty$ gives $K_1^{MF} \propto 2m\Delta^2$

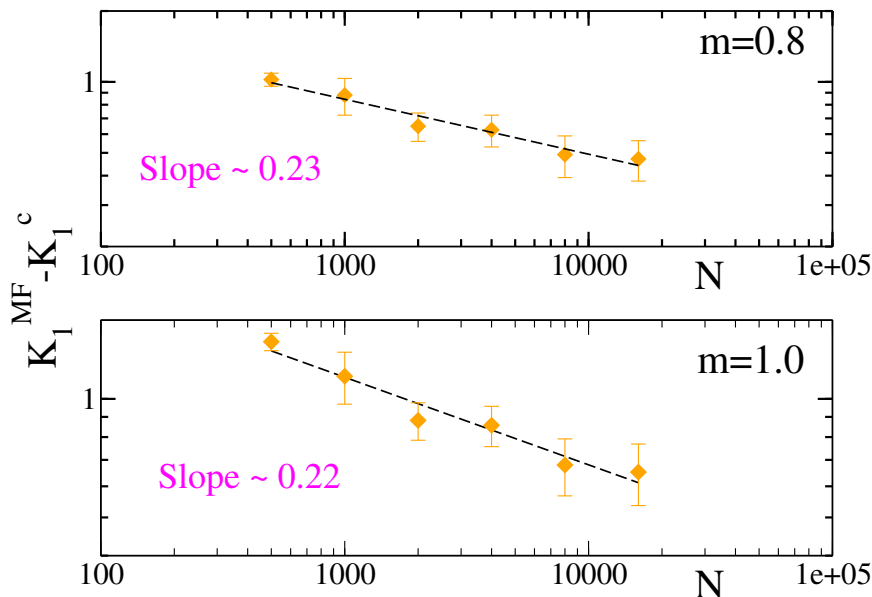
(Acebron et al. PRE (2000); Gupta et al. (PRE 2014))

Finite size effects for K_1^c

If $g(\Omega)$ is an unimodal, symmetric distribution with zero mean

$$\frac{1}{K_1^{MF}} = \frac{\pi g(0)}{2} - \frac{m}{2} \int_{-\infty}^{\infty} \frac{g(\Omega) d\Omega}{1 + m^2 \Omega^2}$$

How to identify the scaling law ruling the approach of $K_1^c(N)$ to its mean-field value for increasing system sizes?



Power-law scaling with the **system size** N for fixed mass

$$K_1^{MF} - K_1^c(N) \propto N^{-1/5}$$

\Rightarrow this is true **for sufficiently low masses**

Mean Field Theory with Noise (Acebrón, Spigler (2008))

ξ_i independent sources of Gaussian white noise

$$\begin{aligned}\dot{\theta}_i &= \nu_i \\ m\dot{\nu}_i &= -\nu_i + \Omega_i + Kr \sin(\phi - \theta_i) + \xi_i\end{aligned}$$

with $\langle \xi_i \rangle = 0$ and $\langle \xi_i(t)\xi_j(t) \rangle = 2D\delta_{ij}\delta(t-s)$

■ Continuum limit (continuity equation for $\rho(\theta, \nu, \Omega, t)$)

$$\frac{\partial \rho}{\partial t} = \frac{D}{m^2} \frac{\partial^2 \rho}{\partial \nu^2} - \frac{1}{m} \frac{\partial}{\partial \nu} [(-\nu + \Omega + Kr \sin(\phi - \theta))\rho] - \nu \frac{\partial \rho}{\partial \theta}$$

■ Normalization $\int_{-\infty}^{\infty} \int_{-\pi}^{\pi} \rho(\theta, \nu, \Omega, 0) d\theta d\nu = 1$

■ Identical oscillators $g(\Omega) = \delta(\Omega)$

Stationary solution $\rho(\theta, \nu) = \chi(\theta)\eta(\nu)$

⇒ It is possible to find frequency and phase distribution from the continuity equation

⇒ K_1^{MF} turns out to be independent of the inertia

Mean Field Theory with Noise

Via averaging the velocity $\nu(t)$ in the long-time limit, the Fokker-Planck equation for the probability distribution $\rho(\theta, \nu, \Omega, t)$ reduces to the Smoluchowski equation

$$\frac{\partial \rho(\theta, t)}{\partial t} = \frac{\partial}{\partial \theta} \left[\left(\frac{\partial V(\theta)}{\partial \theta} + D \frac{\partial \rho(\theta)}{\partial \theta} \right) \left(1 + m \frac{\partial^2 V(\theta)}{\partial \theta^2} \right) \right]$$

with the potential $V(\theta) = -Kr \cos(\theta) - \Omega\theta$. For $D = 0$, the stationary state solution gives

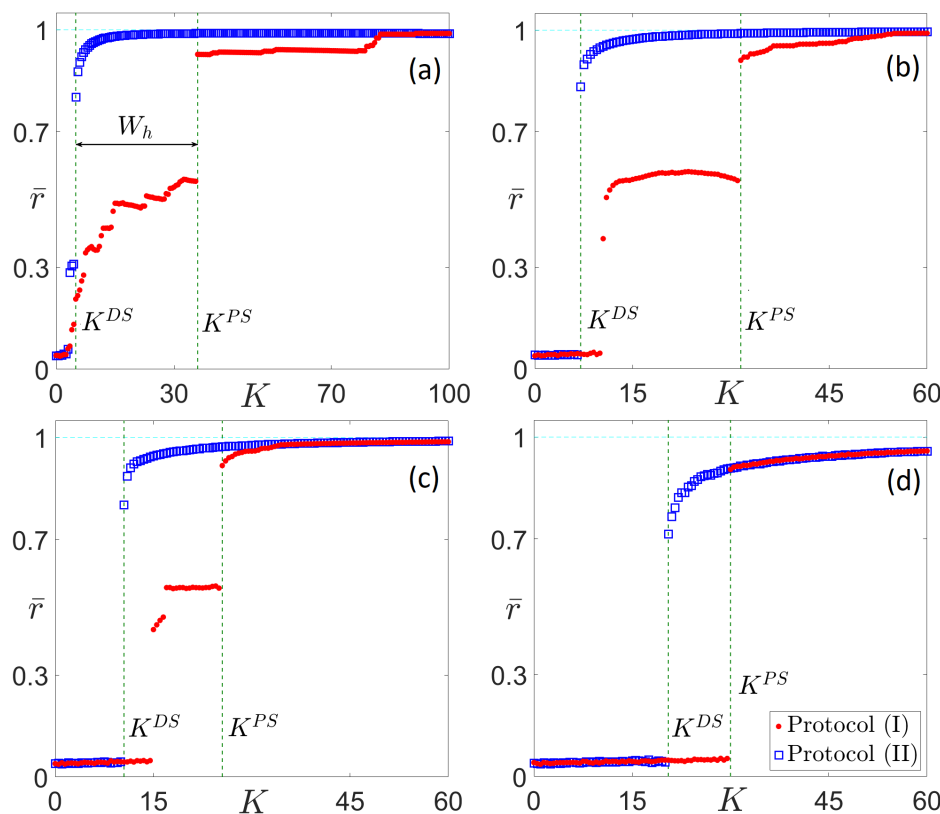
$$r = \left(\frac{\pi}{2} - \frac{m}{2} \right) g(0)Kr + \frac{4}{3}mg(0)(Kr)^2 + \frac{\pi}{16}g''(0)(Kr)^3 + \mathcal{O}(Kr)^4$$

- Drifting and locked oscillators are both contributing to the phase coherence
- The quadratic term $(Kr)^2$ induces hysteresis in the bifurcation diagram
- The hysteresis is reduced with noise
- The critical coupling strength increases monotonically with the increase of D
- The response of phase velocity to external driving is enhanced by a certain amount of noise

Simulations: Noise + Bimodal Frequency Distribution

- Globally coupled network with Bimodal Gaussian frequency distribution
- W_h width of the hysteretic loop, $m = 8$

$$m\ddot{\theta}_i + \dot{\theta}_i = \Omega_i + \frac{K}{N} \sum_j \sin(\theta_j - \theta_i) + \sqrt{2D}\xi_i$$



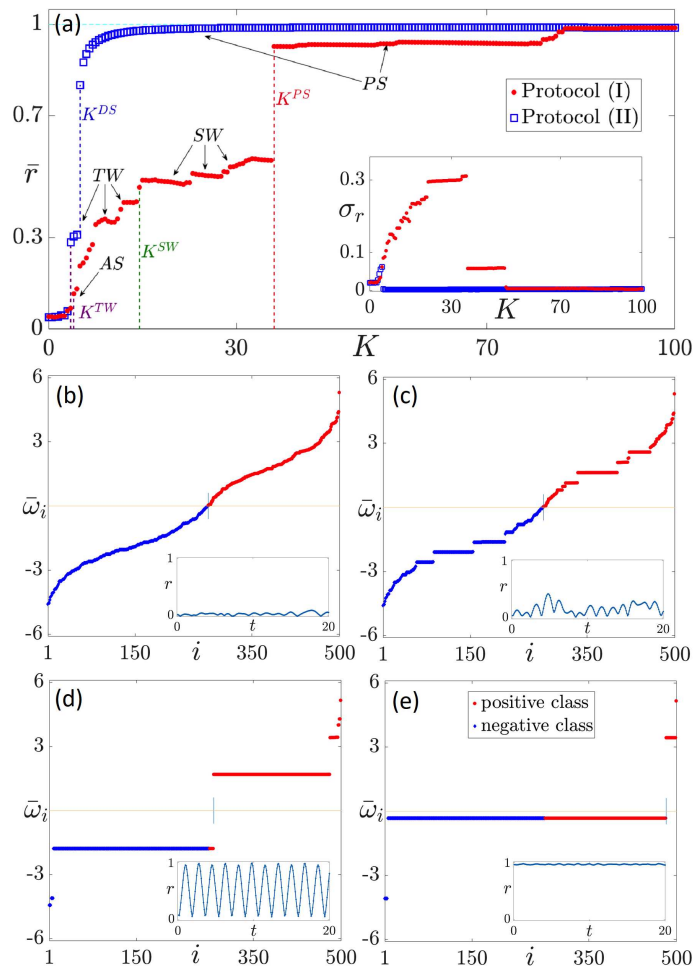
(a) $D=0$; (b) $2D = 9$;
 (c) $2D = 15$; (d) $2D = 30$

- Hysteresis is reduced with noise
- Intermediate states are suppressed

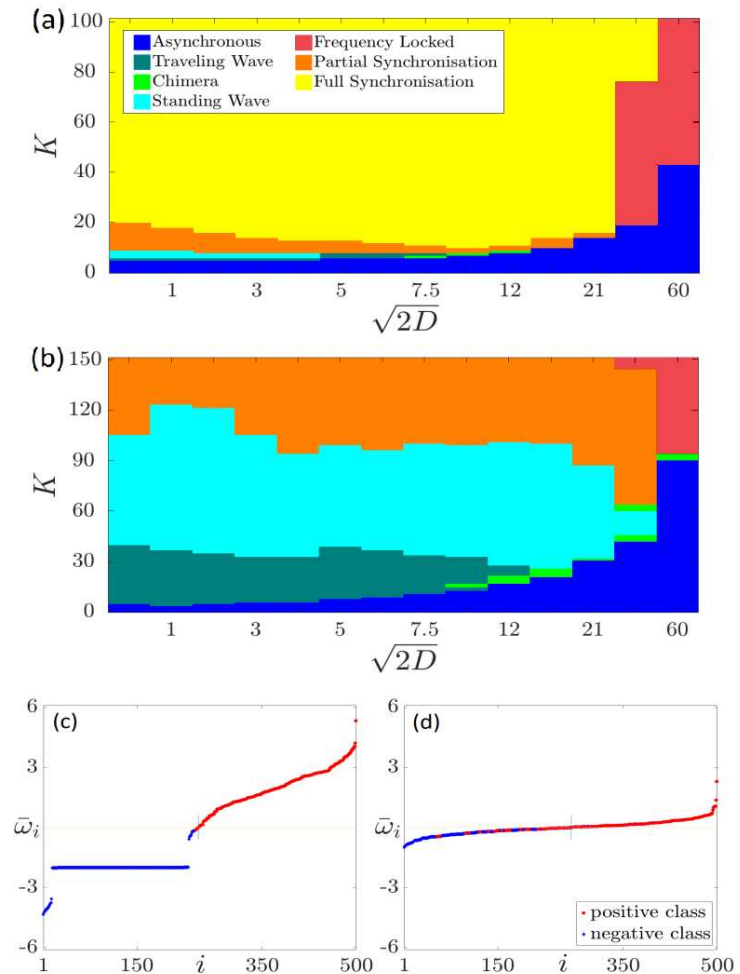
(Tumash et al. (2018))

Simulations: Noise + Bimodal Frequency Distribution

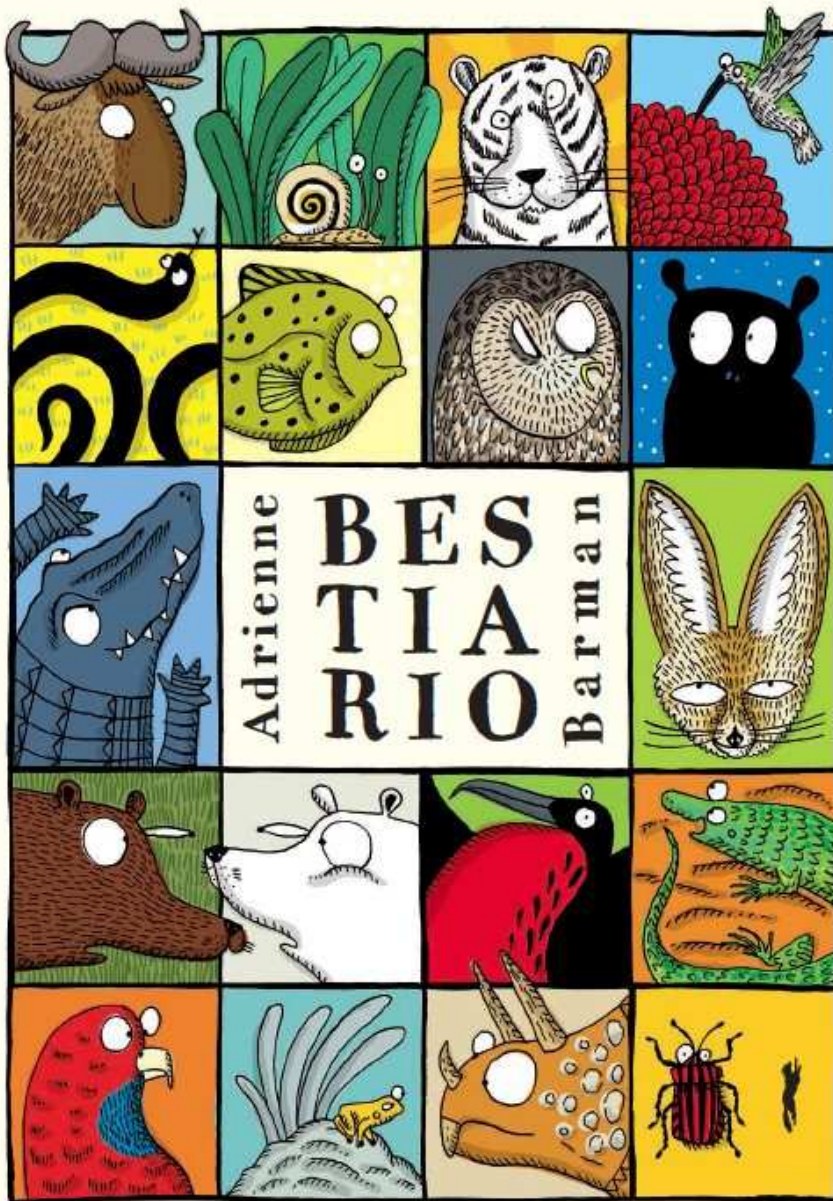
$D = 0, m = 8$



(a) $m = 1$, (b) $m = 30$

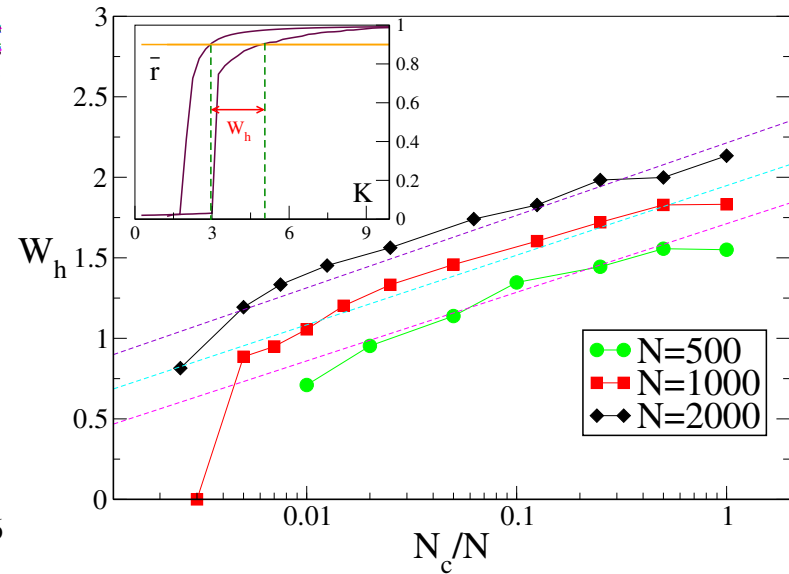
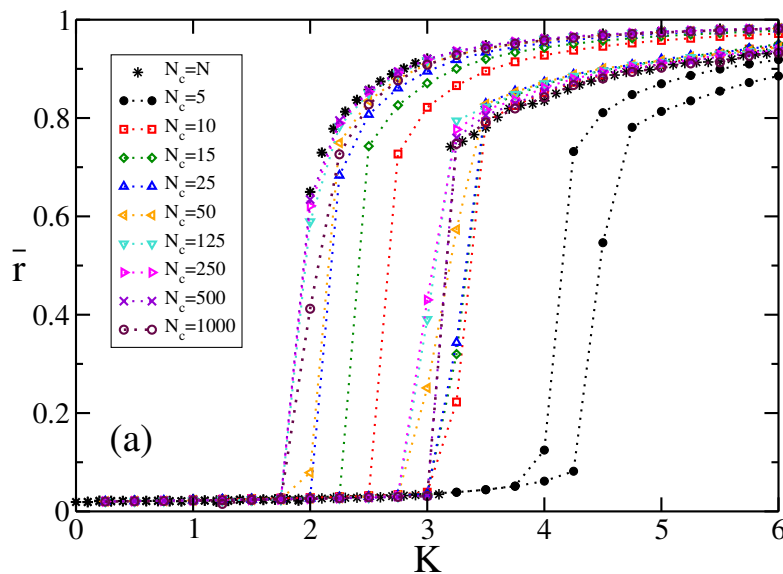


Bestiary



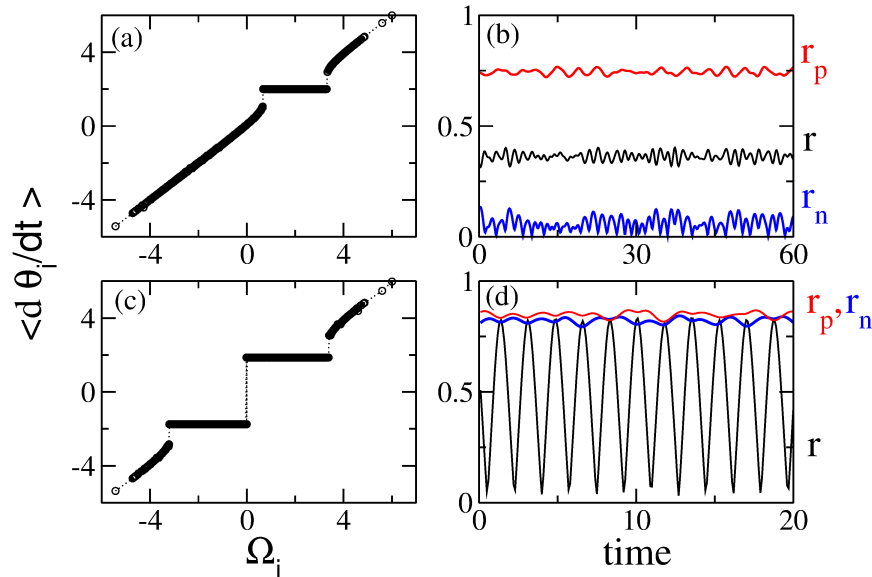
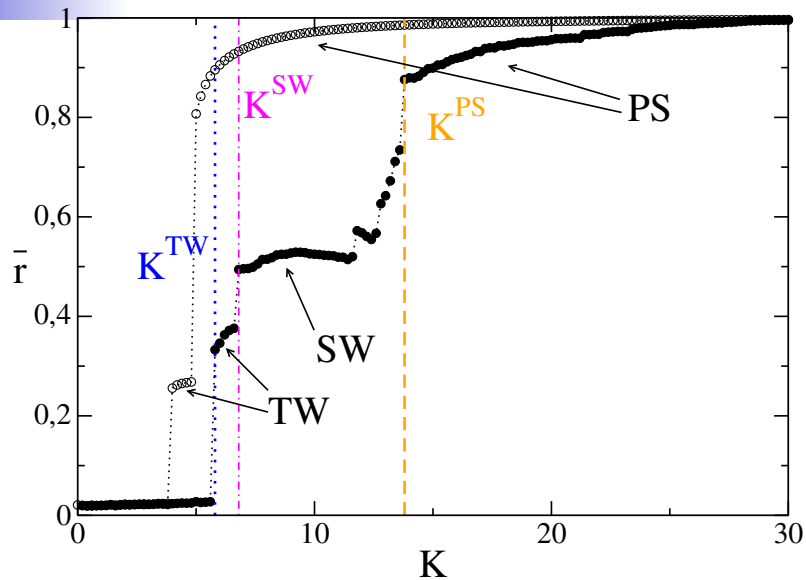
Further works: diluted network + $g(\Omega)$ unimodal

- **Constraint 1** : the random matrix is symmetric
- **Constraint 2** : the in-degree is constant and equal to N_c



- Diluted or fully coupled systems (whenever the coupling is properly rescaled with the in-degree) display **the same phase-diagram**
- For very small connectivities the transition from hysteretic becomes **continuous**
- By increasing the system size the transition **will stay hysteretic** for **extremely small percentages** of connected (incoming) links

Further works: $g(\Omega)$ bimodal

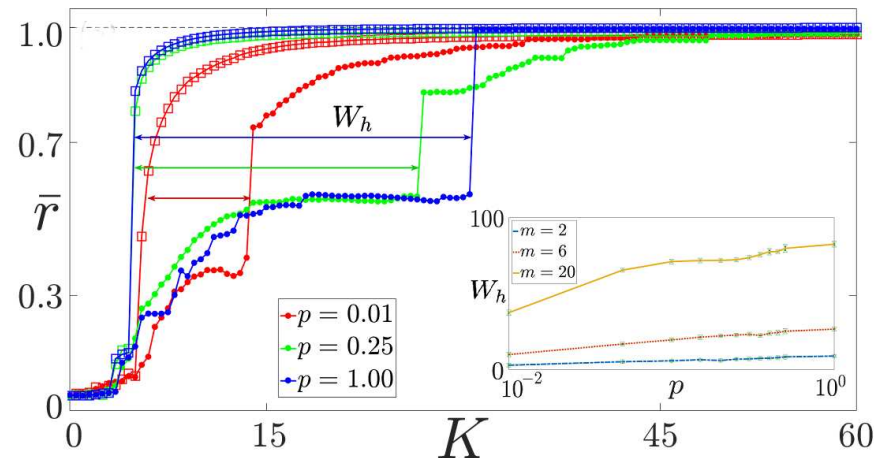
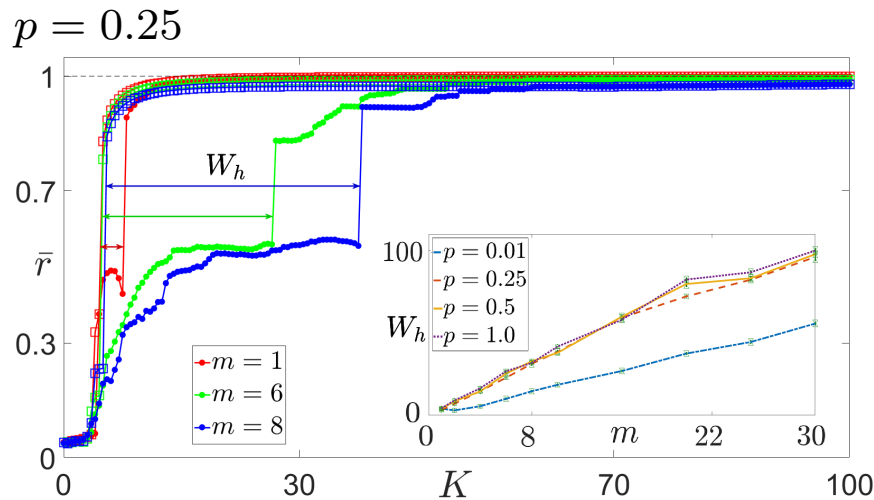


Globally coupled network

- **Traveling Wave (TW)**: a single cluster of oscillators, drifting together with a velocity Ω_0
- **Standing Wave (SW)**: two clusters of drifting oscillators with symmetric opposite velocities $\pm\Omega_0$
- **Partially Synchronized state (PS)**: a cluster of locked rotators with zero average velocity

(Olmi, Torcini (2016))

Further works: diluted network + $g(\Omega)$ bimodal



$m = 6$

- For bigger masses, larger values of critical coupling are required to reach synchronization
- $N_c = pN$
- The hysteretic loop decreases as the network topology becomes more sparse

(Tumash et al. (2018))

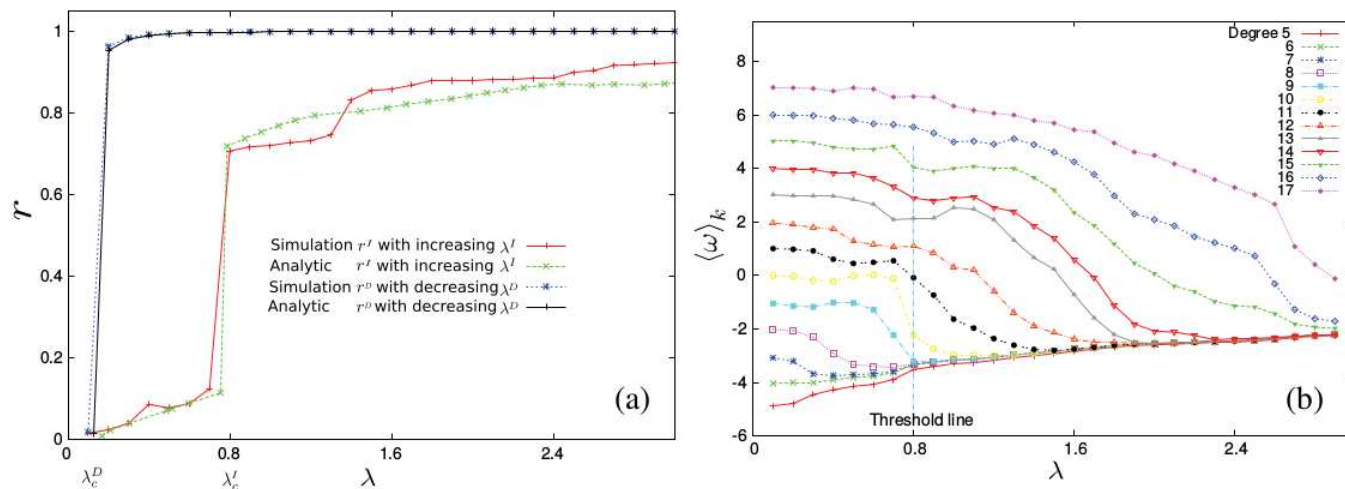
Further works: frequency-degree correlation

Ω_i proportional to its degree with zero mean (so that $\sum_i \Omega_i = 0$): $\Omega_i = B(k_i - \langle k \rangle)$

$$m\ddot{\theta}_i + \dot{\theta}_i = B(k_i - \langle k \rangle) + \lambda \sum_j A_{i,j} \sin(\theta_j - \theta_i)$$

Average frequency $\langle \omega_k \rangle$ of nodes with the same degree k :

$$\langle \omega_k \rangle = \sum_{[i|k_i=k]} \langle \dot{\theta}_i \rangle_t / (NP(k))$$



- Oscillators join the synchronous component grouped into clusters of nodes **with the same degree**
- Small degree nodes synchronize first (**cluster explosive synchronization**)

Further works: chimera state

Two symmetrically coupled populations of N oscillators with inertia

$$m\ddot{\theta}_i^{(\sigma)} + \dot{\theta}_i^{(\sigma)} = \Omega + \sum_{\sigma'=1}^2 \frac{K_{\sigma\sigma'}}{N} \sin(\theta_j^{(\sigma')} - \theta_i^{(\sigma)} - \gamma)$$

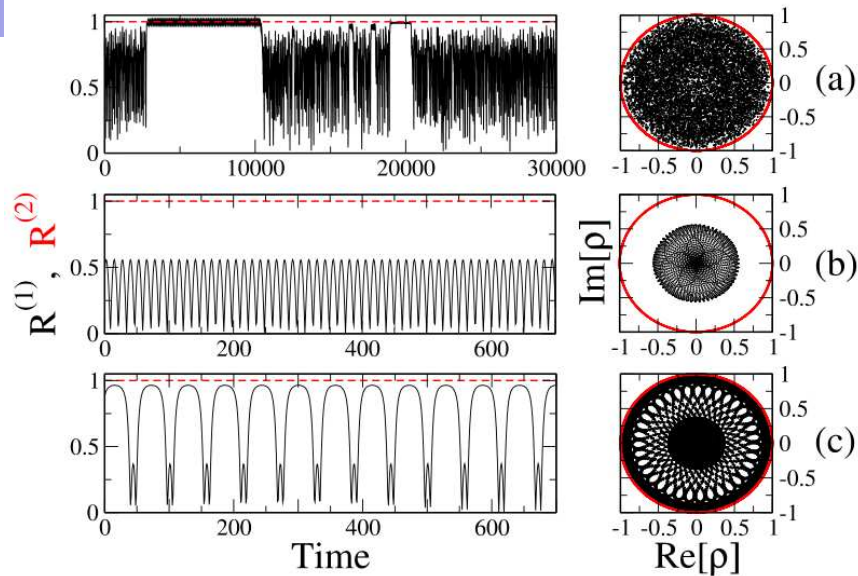
- $\sigma = 1, 2$ identifies the population
- $\theta_i^{(\sigma)}$ is the phase of the i th oscillator in population σ
- Ω is the natural frequency
- $\gamma = \pi - 0.02$ is the fixed frequency lag
- $K_{\sigma,\sigma} > K_{\sigma,\sigma'}$



The collective evolution of each population is characterized in terms of the macroscopic fields $\rho^{(\sigma)}(t) = R^{(\sigma)}(t) \exp[i\Psi(t)] = N^{-1} \sum_{j=1}^N \exp[i\theta_j^{(\sigma)}(t)]$.

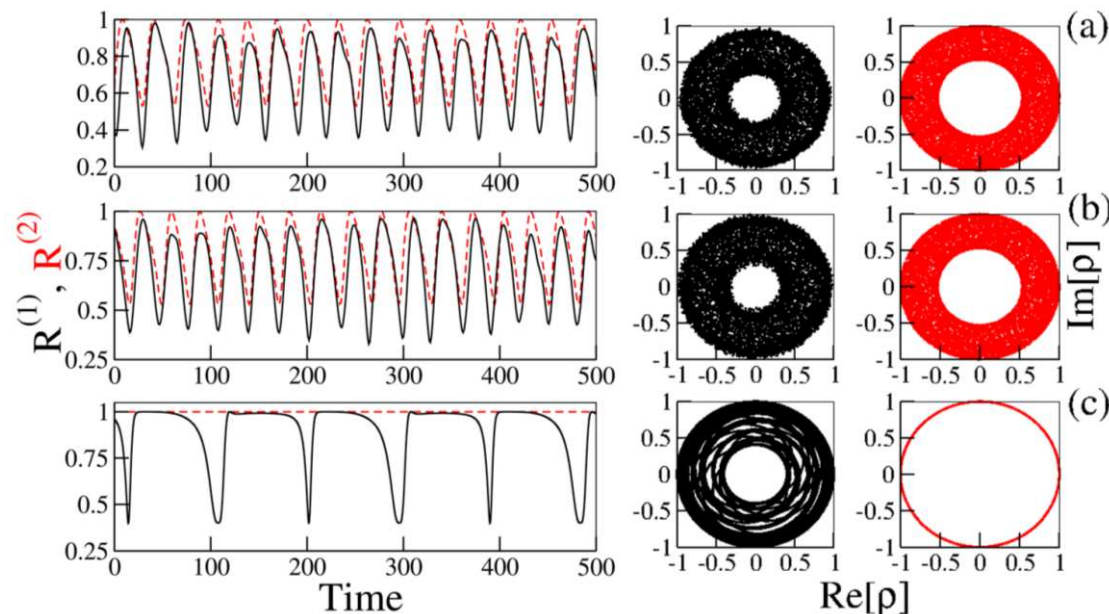
In analogy with [Abrams, Mirollo, Strogatz and Wiley, PRL \(2008\)](#).

Further works: chimera state



Broken symmetry initial conditions

- $m = 10$ intermittent chaotic chimera
- $m = 3$ breathing chimera
- $m = 10^{-4}$ quasi-periodic chimera



Uniform initial conditions

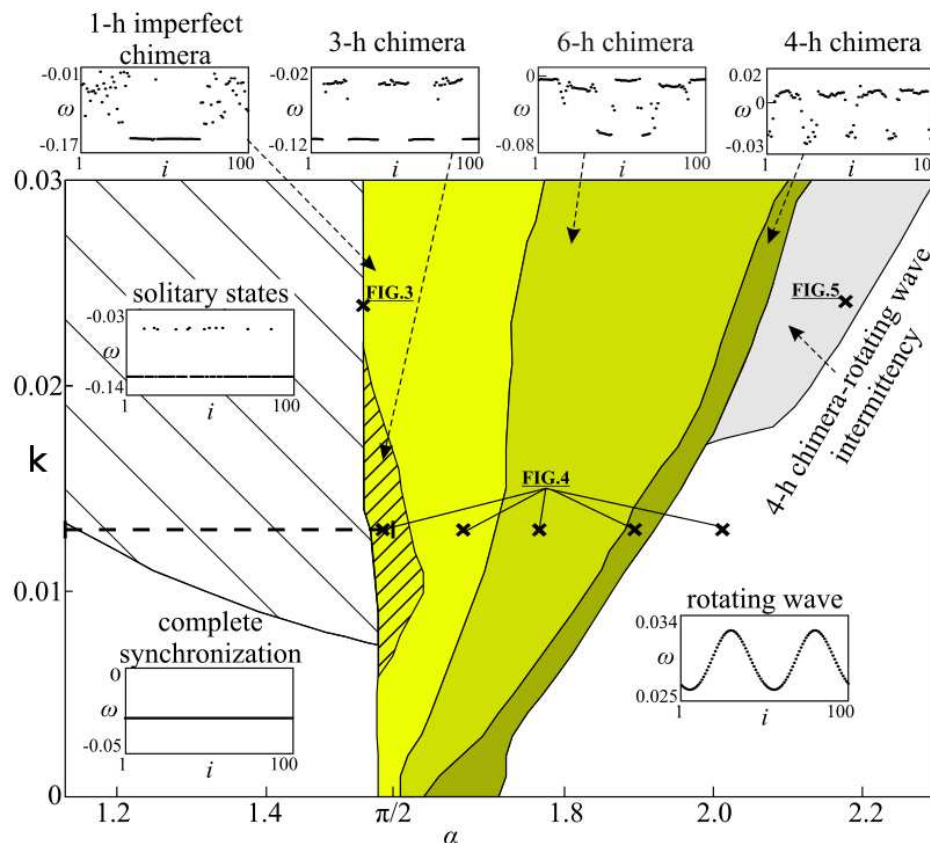
- $m = 10, 9$ chaotic 2 populations states
- $m = 3$ chaotic chimera

(Olmi et al. (2015))

Further works: imperfect chimera state

A ring of N non-locally coupled Kuramoto oscillators with inertia, each one connected to its P nearest neighbours to the left and to the right with equal strength

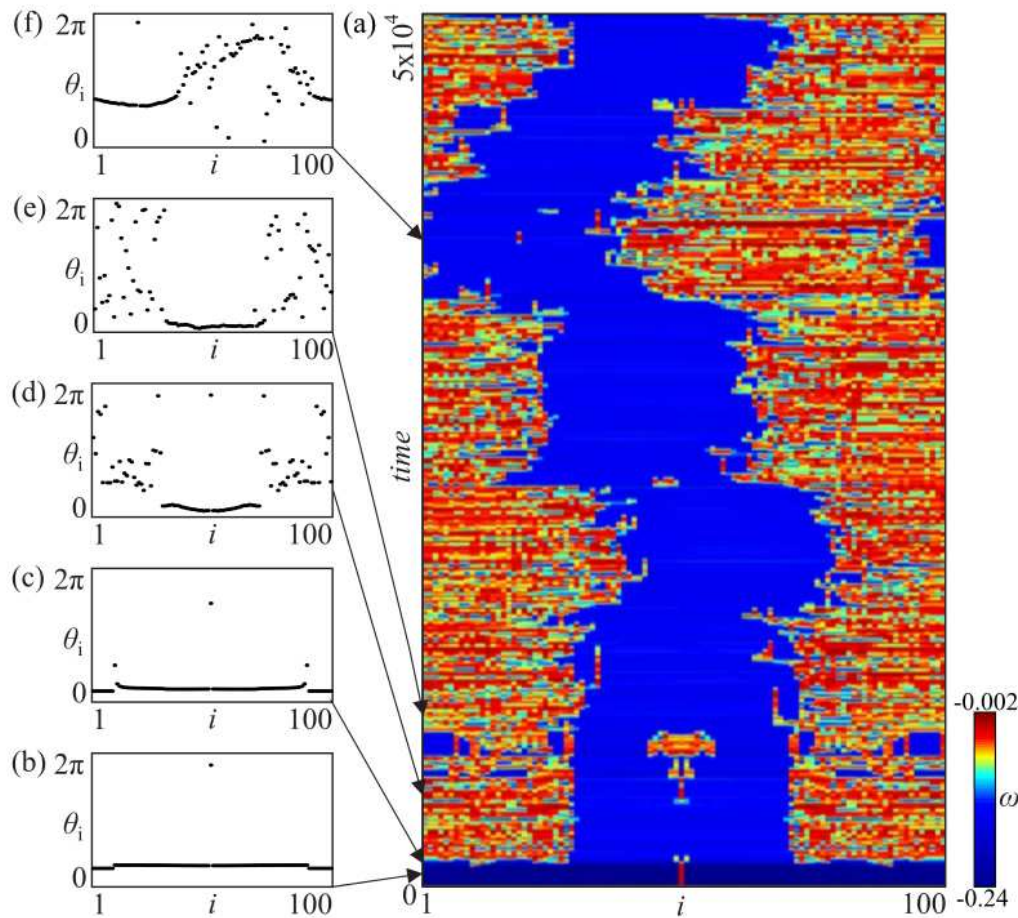
$$m\ddot{\theta}_i + \epsilon\dot{\theta}_i = \frac{k}{2P+1} \sum_{j=i-P}^{i+P} \sin(\theta_j - \theta_i - \alpha)$$



- The system is multistable
- Imperfect chimera state: a certain number of oscillators split from synchronized domain

(Jaros et al. (2015))

Further works: imperfect chimera state



- The creation of chimera states is characterized by the appearance of **solitary states**
- Separation of successive elements, along with time, creates imperfect chimera
- Chimeras is **perfect** only for a certain time

(Jaros et al. (2015))

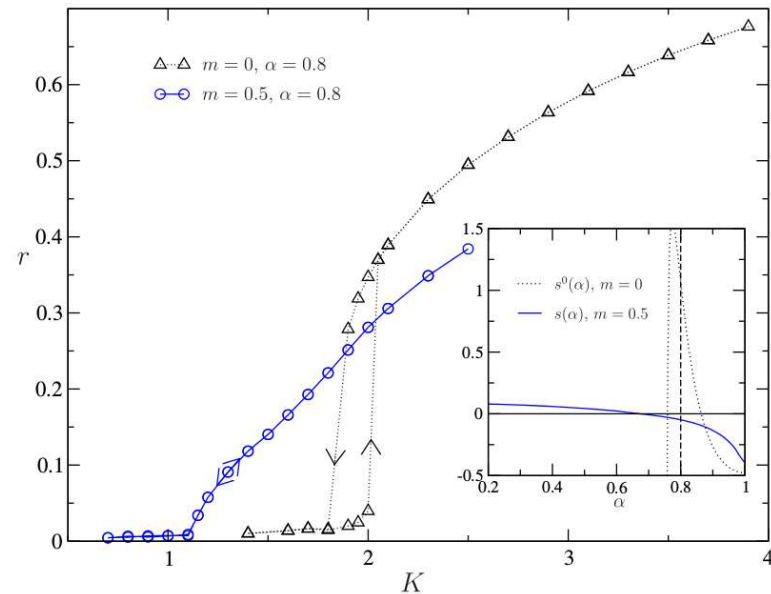
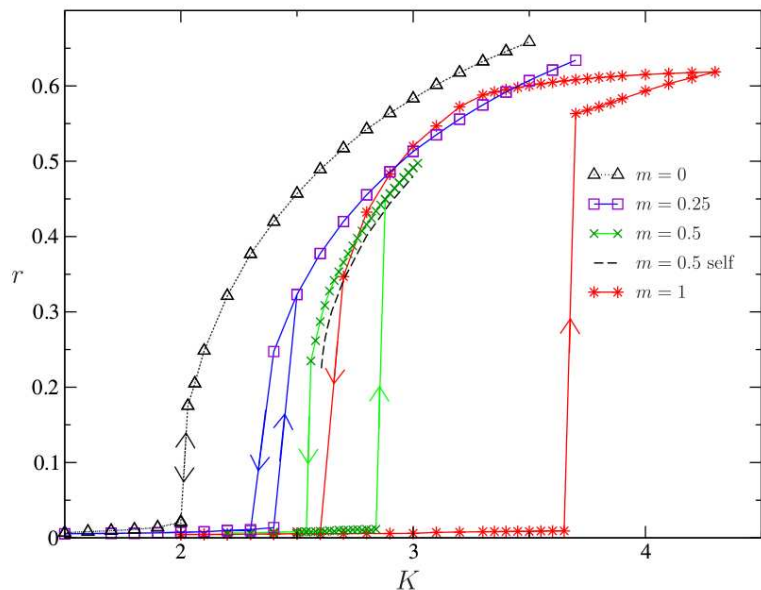
Further works: frustration parameter

Any amount of inertia, however small, can act both ways: it can turn discontinuous an otherwise continuous transition and the other way around

$$\dot{\theta}_i = \nu_i$$

$$m\dot{\nu}_i = \gamma(\Omega_i - \nu_i) + \frac{K}{N} \sum_{j=1}^N \sin(\theta_j - \theta_i - \alpha)$$

with $g(-\Omega) = g(\Omega) = \frac{\sigma}{\pi} \frac{1}{\sigma^2 + \Omega^2}$, where $\sigma = 1$



Applications

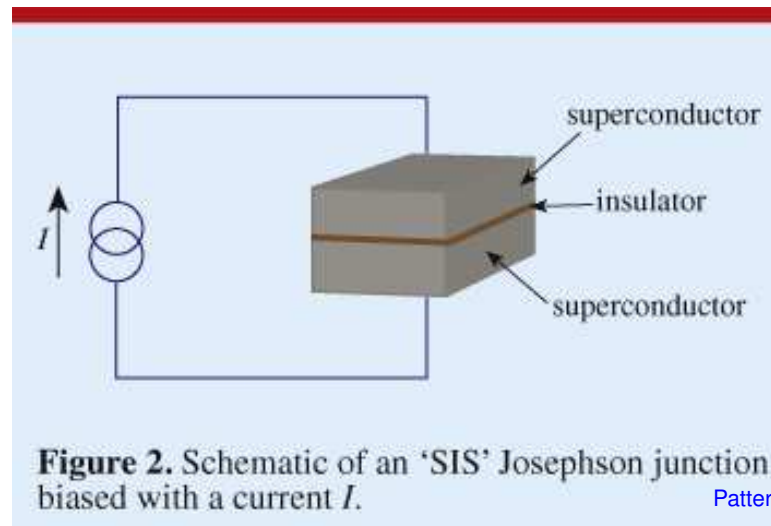
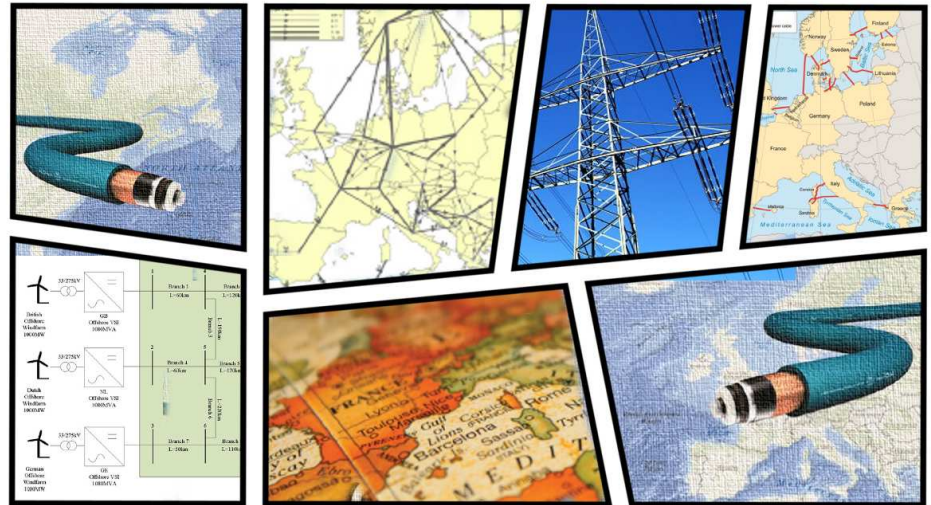


Figure 2. Schematic of an 'SIS' Josephson junction biased with a current I .

Power Plants

Power

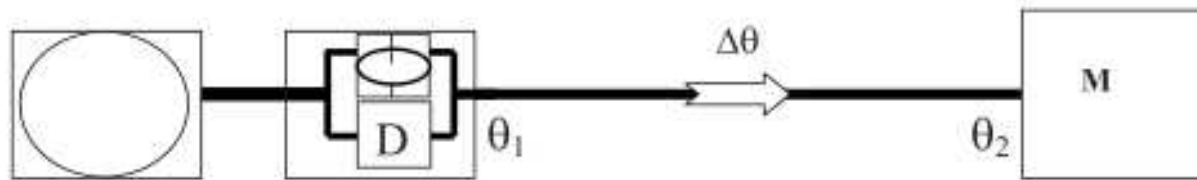


Fig. 1. Equivalent diagram of generator and machine connected by a transmission line. The turbine consists of a flywheel and dissipation D .

- A power plant consists of a **boiler** producing a **constant** power, as well as a **turbine** (generator) with high inertia and some damping.
- Transmitted power through a line: $P_{12}^{max} \sin(\theta_2 - \theta_1)$.
- Power plant + transmission line = **power source that feeds energy into the system**. This energy can be **accumulated** as **rotational energy** or **dissipated** due to **friction**.
- The remaining part is available for a **user** (the machine M), provided that there exists a **phase angle difference** $\Delta\theta = \theta_2 - \theta_1$ between the two mechanical rotators (phase shift is necessary for ac power transmission)

Power grids: swing equation

Power flow analysis can be described in terms of the phase angles θ'_s that characterize both the **rotor dynamics** (and hence the energy stored or dissipated) and the **power flow** between any two rotors connected by an ac line.

$$\theta_i(t) = \Omega t + \phi_i(t), \quad \Omega = 2\pi \times 50Hz$$

$$P_i^{source} = P_i^{diss} + P_i^{acc} + P_i^{transmitted}$$

$$P_i^{diss} = k_i^D \dot{\theta}_i^2, \quad P_i^{acc} = \frac{1}{2} I_i \frac{d^2 \theta_i}{dt^2}, \quad P_i^{transmitted} = P_{ij}^{max} \sin(\theta_j - \theta_i)$$

Assuming only slow phase changes compared to the frequency ($|\dot{\theta}_i| \ll \Omega$)

$$I_i \Omega \ddot{\phi}_i = P_i^{source} - k_i^D \Omega^2 - 2k_i \Omega \dot{\phi} + \sum_j P_{ij}^{max} \sin(\theta_j - \theta_i)$$

only the phase difference between the elements of the grid matters!

(Filatrella et al. (2008))

Power grids: parameters

Every element i is described by the same rescaled equation of motion with a parameter P_i giving the generated ($P_i > 0$) or consumed ($P_i < 0$) power

$$\frac{d^2 \phi_i}{dt^2} = P_i - \alpha_i \frac{d\phi}{dt} + \sum_j K_{ij} \sin(\theta_j - \theta_i)$$

where $K_{ij} = \frac{P_{ij}^{max}}{I_i \Omega}$, $P_i = \frac{P_i^{source} - k_i^D \Omega^2}{I_i \Omega}$, $\alpha_i = \frac{2k_i}{I_i}$, $\sum_j P_j = 0$.

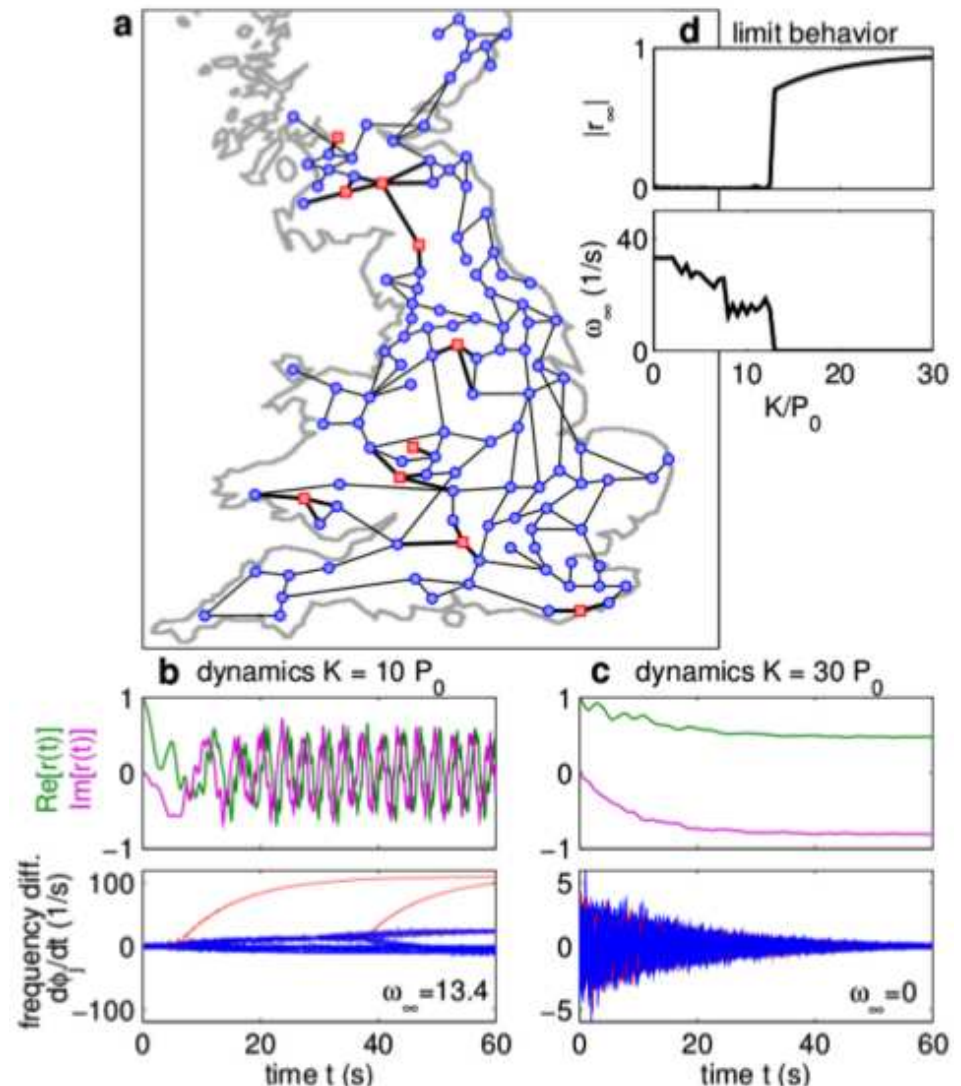
- Large centralized power plants generating $P_i^{source} = 100Mw$ each
- Each synchronous generator has a moment of inertia of $I_i = 10^4 kgm^2$
- The mechanically dissipated power $k_i^D \Omega^2$ usually is a small fraction of P^{source}
- Additional sources of dissipation are not taken into account
- A transmission capacity for major overhead power line is up to $P_{ij}^{max} = 700MW$
- The transmission capacity for a line connecting a small city is $K_{ij} \leq 10^2 s^2$
- $\alpha_i = 0.1s^{-1}$, $P_i = 10s^{-2}$ for large power plants, $P_i = -1s^{-2}$ for a small city

Power Grids (Rohden et al. (2012))

- Larger networks of complex topologies equally exhibit **coexistence** with power outage and **self-organized synchrony**
- Average frequency difference

$$\omega = \sum_j |d\phi_j/dt|/N$$
- Order parameter

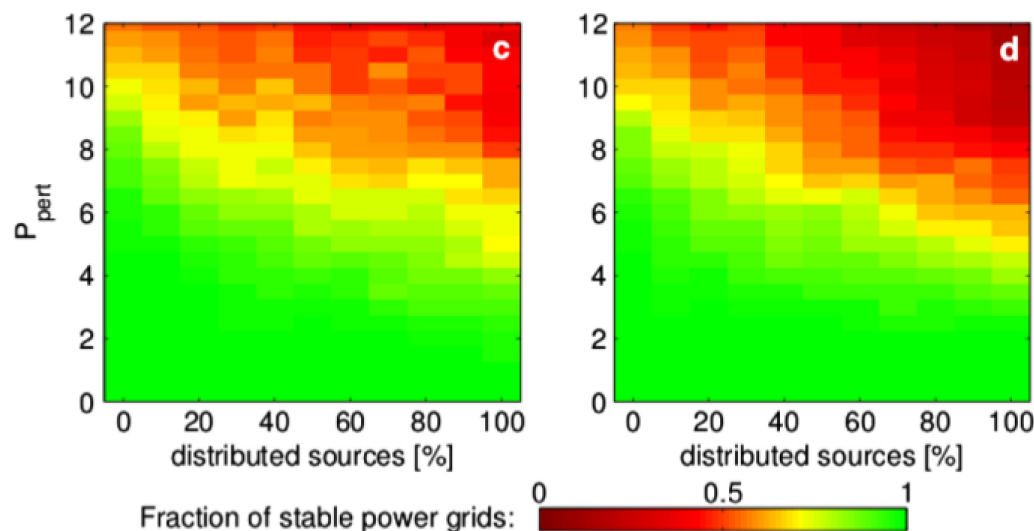
$$r(t) = \sum_j e^{i\phi_j(t)}/N$$
- Topology of the British power grid: **120** nodes and **165** transmission lines; **10** power plants (randomly chosen) and **110** consumers
- Power plants are connected to their neighbors with a higher capacity cK



Power Grids Stability (Rohden et al. (2012))

How does decentralization impact the system's stability to dynamic perturbations?

- Replace large power plants ($P_j = 11P_0$) by smaller ones ($P_j = 1.1P_0$).
- Test the **stability against fluctuations** by transiently increasing the power demand of each consumer during a short time interval (the condition $\sum_j P_j = 0$ is violated)
- After the perturbation is **switched off**, the system either relaxes back to a steady state or does not, depending on the strength of the perturbation
- The maximally allowed perturbation strength **shrinks with decentralization**, but still all grids are stable up to strengths a few times larger than the unperturbed load



Josephson Junctions

- The Josephson effect is the phenomenon of **supercurrent**, a current that flows indefinitely long without any voltage applied, through a **Josephson junction (JJ)**
- A JJ consists of two or more superconductors coupled by a weak link, which can consist of a thin insulating barrier, a short section of non-superconducting metal, or a physical constriction that weakens the superconductivity at the point of contact
- The Josephson effect is an example of a macroscopic quantum phenomenon, predicted by Brian David Josephson in 1962 ([Josephson \(1962\)](#))
- The DC Josephson effect had been seen in experiments prior to 1962, but had been attributed to “super-shorts” or **breaches** in the insulating barrier
- The first paper to claim the discovery of Josephson’s effect, and to make the requisite experimental checks, was that of ([Anderson and Rowell \(1963\)](#))
- Before JJ, it was only known that normal, non-superconducting electrons can flow through an insulating barrier (**quantum tunneling**). Josephson first predicted the tunneling of superconducting Cooper pairs ([Nobel Prize in Physics 1973](#)).

A locally coupled Kuramoto model with inertia can be derived from a coupled resistively and capacitively shunted junction eqs for an underdamped ladder with periodic boundary conditions ([Trees et al. \(2005\)](#)): good agreements are achieved for phase and frequency synchronization

References

- B. Ermentrout, *Journal of Mathematical Biology* 29 , 571 (1991)
- EE. Hanson, *Cellular Pacemakers*, ed. D.O. Carpenter, Vol. 2 (Wiley, New York, 1982)
pp. 81-100
- S. H. Strogatz, *Nonlinear Dynamics And Chaos: With Applications To Physics, Biology, Chemistry, And Engineering*, 1st Edition, Westview Press (1994)
- B. R. Trees, V. Saranathan, D. Stroud, *Physical Review E* 71 (1) (2005) 016215
- G. Filatella, A. H. Nielsen, N. F. Pedersen, *The European Physical Journal B* 61 (4), 485-491 (2008)
- H. D. Chiang, *BCU Methodologies, and Applications*, John Wiley & Sons (2011)
- M. Levi, F. C. Hoppensteadt, W. L. Miranker, *Quarterly of Applied Mathematics* 36.2, 167-198 (1978)
- H. A. Tanaka, A. J. Lichtenberg, S. Oishi, *Physical Review Letters* 78 (11) (1997)
2104-2107 (1997)
- S. Olmi, A. Navas, S. Boccaletti, A. Torcini, *Physical Review E* 90 (4), 042905 (2014)
- S. Gupta, A. Campa, S. Ruffo, *Physical Review E* 89 (2) 022123 (2014)
- J. A. Acebrón, L. L. Bonilla, R. Spigler, *Physical Review E* 62 (3) 3437-3454 (2000)
- J. A. Acebrón, R. Spigler, *Physical Review Letters* 81 (11) 2229-2232 (2008)

References

- H. Hong, M. Choi, B. Yoon, K. Park, K. Soh, *Journal of Physics A: Mathematical and General* 32 (1) L9 (1999)
- L. L. Bonilla, *Physical Review E* 62 (4), 4862-4868 (2000)
- H. Hong, M. Y. Choi, *Physical Review E* 62 (5) (2000) 6462-6468
- L. Tumash, S. Olmi, E. Schöll, *EPL* 123, 20001 (2018)
- S. Olmi, A. Torcini, in *Control of Self-Organizing Nonlinear Systems*, 25-45 (2016)
- P. Ji, T. K. D. Peron, P. J. Menck, F. A. Rodrigues, J. Kurths, *Physical Review Letters* 110 (21), 218701 (2013)
- S. Olmi, E. A. Martens, S. Thutupalli, A. Torcini, *Physical Review E* 92 (3) 030901 (2015)
- P. Jaros, Y. Maistrenko, T. Kapitaniak, *Physical Review E* 91 (2) 022907 (2015)
- J. Barré, D. Métivier, *Physical review letters* 117.21, 214102 (2016)
- M. Rohden, A. Sorge, M. Timme, D. Witthaut, *Physical Review Letters* 109 (6), 064101 (2012)
- B. D. Josephson, *Physics letters* 1 (7): 251-253 (1962)
- P. W. Anderson, J. M. Rowell, *Physical Review Letters* 10 (6): 230 (1963)

Extension of the Mean Field Theory

In principle one could fix the discriminating frequency to some arbitrary value Ω_0 and solve self-consistently

$$r = r_L + r_D$$

$$r_L^{I,II} = Kr \int_{-\theta_0}^{\theta_0} \cos^2 \theta g(Kr \sin \theta) d\theta \quad r_D^{I,II} \simeq -mKr \int_{-\Omega_0}^{\infty} \frac{1}{(m\Omega)^3} g(\Omega) d\Omega$$

This amounts to obtain a solution $r^0 = r^0(K, \Omega_0)$ by solving

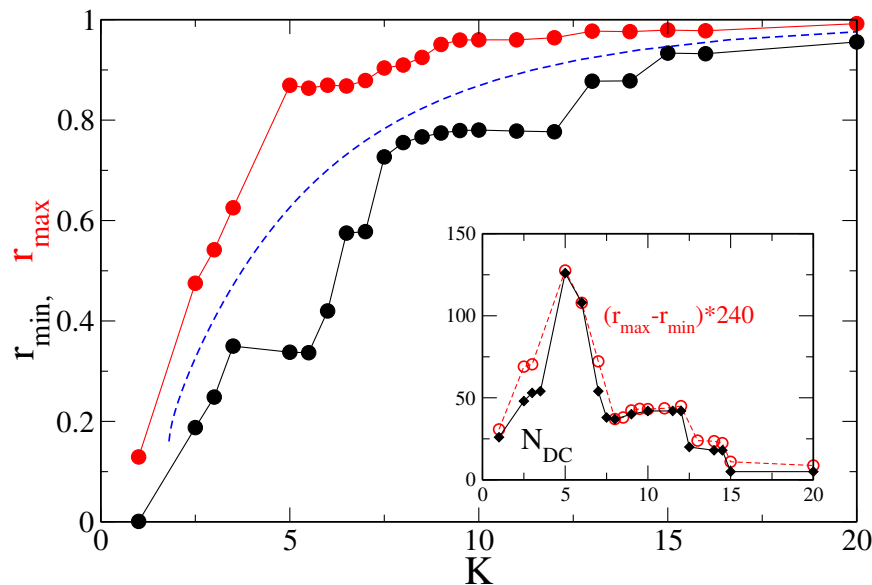
$$\int_{-\theta_0}^{\theta_0} \cos^2 \theta g(Kr^0 \sin \theta) d\theta - m \int_{-\Omega_0}^{\infty} \frac{1}{(m\Omega)^3} g(\Omega) d\Omega = \frac{1}{K}$$

with $\theta_0 = \sin^{-1}(\Omega_0/Kr^0)$. The solution exists if $\Omega_0 < \Omega_D = Kr^0$.

\Rightarrow A portion of the (K, r) plane delimited by the curve $r^{II}(K)$ is filled with the curves $r^0(K)$ obtained for different Ω_0 values.

Drifting Clusters (Olmi et al. (2014))

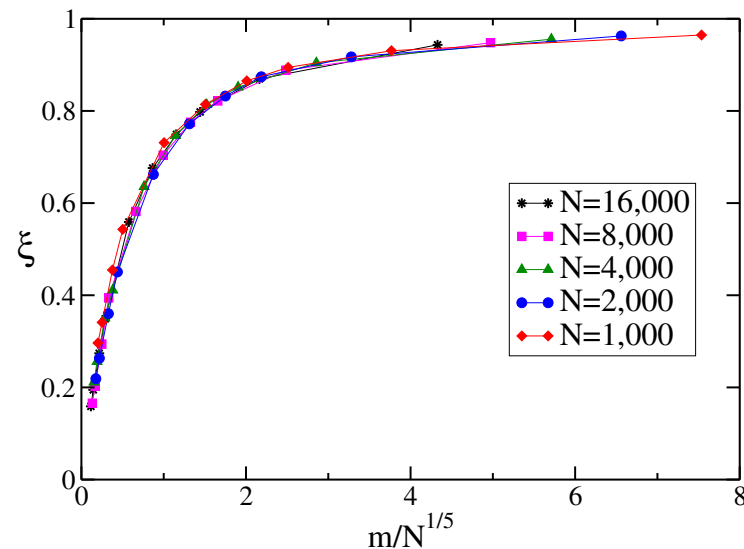
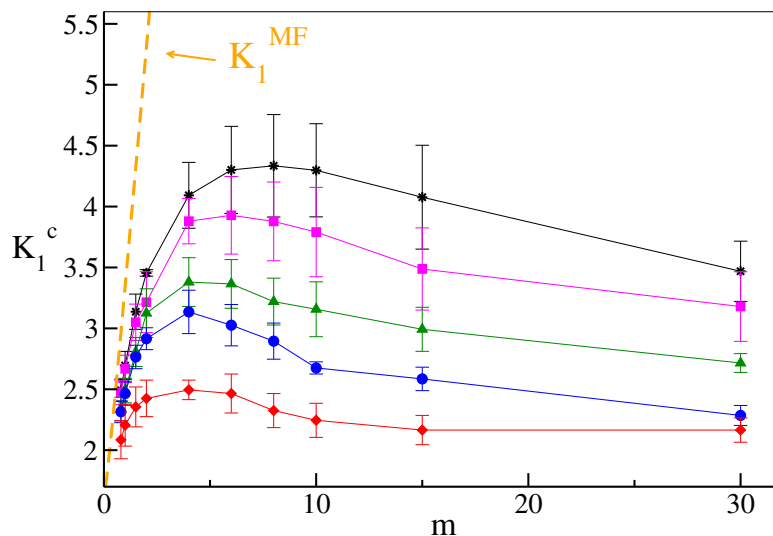
- The amplitude of the oscillations of $r(t)$ and the number of oscillators in the drifting clusters N_{DC} correlates in a linear manner
- The oscillations in $r(t)$ are induced by the presence of large secondary clusters characterized by finite whirling velocities
- At smaller masses oscillations are present, but reduced in amplitude. Oscillations are due to finite size effects since no clusters of drifting oscillators are observed



- Blue dashed line \Rightarrow estimated mean field value r^I by Tanaka et al. (1997)
- The mean field theory captures the average increase of the order parameter but it does not foresee the oscillations

Dependence On the Mass K_1^c

- K_1^c increases with m up to a maximal value and then decreases at larger masses
- by increasing N K_1^c increases and the position of the maximum shifts to larger masses (finite size effects)

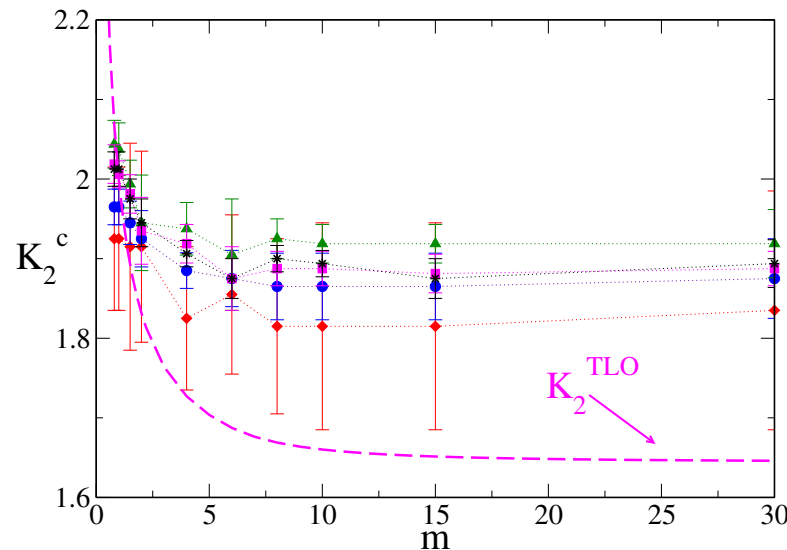


The following general scaling seems to apply

$$\xi \equiv \frac{K_1^{MF} - K_1^c(m, N)}{K_1^{MF}} = G\left(\frac{m}{N^{1/5}}\right) \quad \text{where } K_1^{MF} \propto 2m \text{ for } m > 1$$

Dependence On the Mass K_2^c

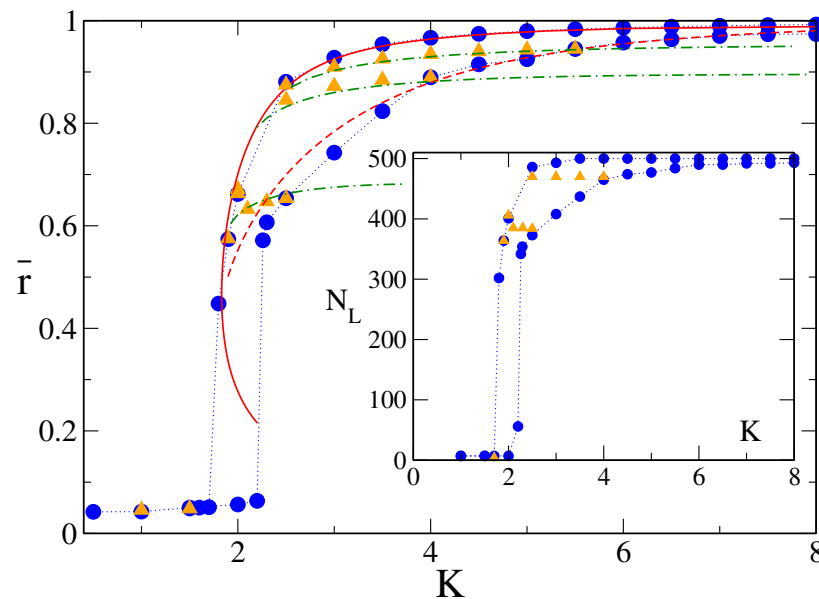
The TLO approach fails to reproduce the critical coupling for the transition from asynchronous to synchronous state (i.e., K_1^c), however it gives a good estimate of the return curve obtained with protocol II from the synchronized to the asynchronous regime



- K_2^c initially decreases with m then saturates, limited variations with the size N
- K_2^{TLO} is the minimal coupling associated to a partially synchronized state given by TLO approach for protocol II
- K_2^{TLO} exhibits the same behaviour as K_2^c , however it slightly underestimates the asymptotic value (see the scale)

Further works: diluted network

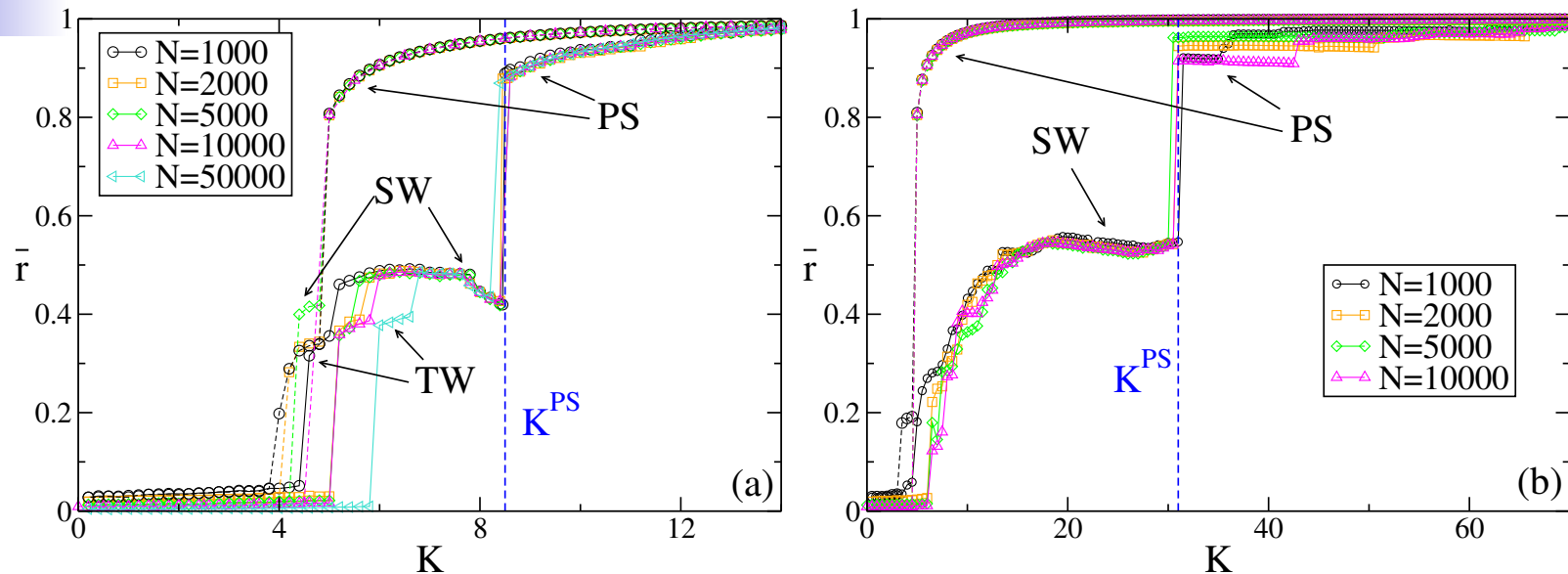
- The TLO mean field theory still gives reasonable results (70% of broken links)
- All the states between the synchronization curves obtained following Protocol I and II are reachable and stable



- These states, located in the region between the synchronization curves, are characterized by a frozen cluster structure, composed by a constant N_L
- The generalized mean-field solution $r^0(K, \Omega_0)$ is able to well reproduce the numerically obtained paths connecting the synchronization curves (I) and (II)

Further works: $g(\Omega)$ bimodal

Finite size effects



Small inertia value

- K^{TW} and K^{SW} increase with N
- The transition value K^{PS} and K^{DS} seem independent from N
- In the thermodynamic limit TW and SW will be no more visited (the incoherent state will lose stability at K^{SW})

Large inertia value

- The transition to **SW** occurs via the emergence of clusters

Italian High Voltage Power Grid



Each node is described by the phase:

$$\phi_i(t) = \omega_{AC}t + \theta_i(t)$$

where $\omega_{AC} = 2\pi \cdot 50 \text{ Hz}$ is the standard AC frequency and θ_i is the phase deviation from ω_{AC} .

Consumers and generators can be distinguished by the sign of parameter P_i :

$$P_i > 0 \quad (P_i < 0)$$

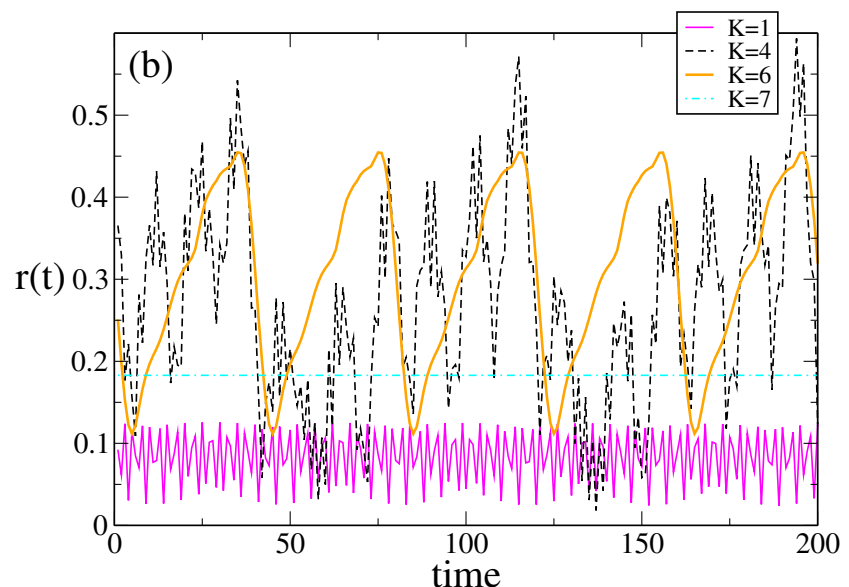
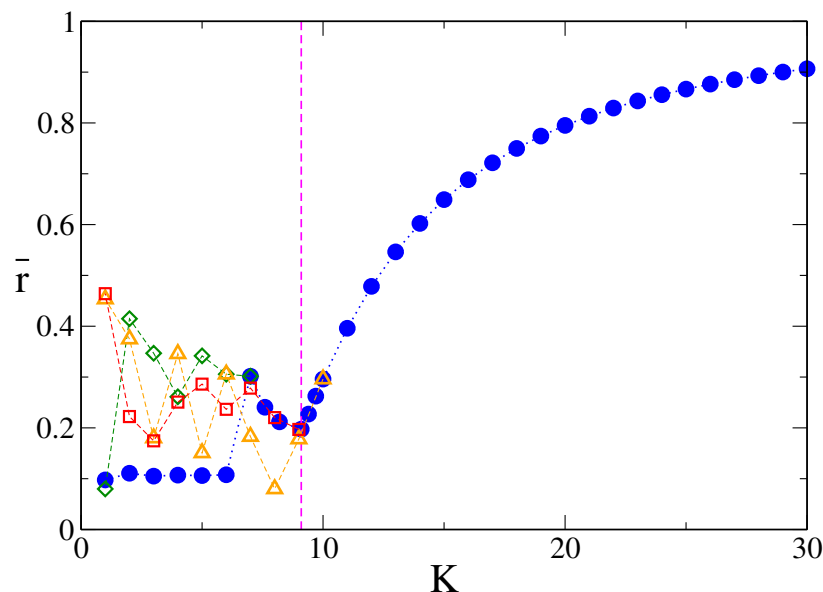
corresponds to **generated** (**consumed**) power.

$$\ddot{\theta}_i = \alpha \left[-\dot{\theta}_i + P_i + K \sum_{ij} C_{i,j} \sin(\theta_j - \theta_i) \right]$$

Average connectivity $\langle N_c \rangle = 2.865$

Italian High Voltage Power Grid

- We do not observe any hysteretic behavior or multistability down to $K = 9$
- For smaller coupling an intricate behavior is observable depending on initial conditions
- Generators and consumers compete in order to oscillates at different frequencies
- The local architecture favours a splitting based on the proximity of the oscillators
- Several small whirling clusters appear characterized by different phase velocities
- The irregular oscillations in $r(t)$ reflect quasi-periodic motions



Italian High Voltage Power Grid

By following Protocol II

- the system stays in **one** cluster up to $K = 7$
- at $K = 6$ wide oscillations emerge in $r(t)$ due to the locked clusters that have been splitted in two (is this also the origin for the emergent multistability?)
- By lowering further K several whirling small clusters appear and r becomes irregular

